CO-PRECIPITATION AS A TOOL FOR EFFECTIVE DOPING OF MAGNESIUM IN ZINC OXIDE: STUDIES ON STRUCTURAL, OPTICAL AND PHOTOCATALYTIC PROPERTIES

U. Sachin Varma[1], P. Gautham[1], D.V. Ravi Kumar[1], K. M. Sreekanth[1,*], G. Sivasubramanian[1] and K. M. Sreedhar[2]

[1]Department of Sciences, Amrita School of Engineering, Amrita Vishwa Vidyapeetham, Coimbatore, India - 641112
[2]Department of Chemistry, Amrita School of Arts & Sciences, Amrita Vishwa Vidyapeetham, Amritapuri, India - 690525
*E-mail : km_sreekanth@cb.amrita.edu

ABSTRACT

Elimination of toxic compounds from our essential commodities such as water, air, foods etc. and provision for safe and clean basic needs is currently one of the most significant international topics for research, especially in food, water and air pollution control. Metal oxides have emerged as one of the most interesting materials in the current period owing to their potential catalytic properties. The II-VI metal oxides are gaining considerable attention in optoelectronics and in rectifying environmental issues due to their ability to produce charge carriers when accelerated with a sufficient amount of energy. The electronic structure, fluorescence and phosphorescence properties and charge transport abilities of the metal oxides have made them photo catalysts. In this paper, we report a precise investigation of structural, optical and photo catalytic properties of industrially and technologically important ZnO and $Mg_xZn_{(1-x)}O$ nanoparticles. The materials were synthesized via chemical methods using solutions of zinc sulphate, sodium hydroxide, silver nitrate and magnesium sulphate. The structural, optical and photocatalytic properties of the synthesized samples were studied using X-ray diffractometer and UV-VIS spectrophotometer. The average crystallite size of the prepared samples is between 15 to 20 nm. The optical band value of the ZnO nanoparticles was found 3.3 eV. The photocatalytic studies were conducted using an in-house built assembly and photocatalytic degradation of Cr was chosen as a reference. The synthesized $Mg_xZn_{(1-x)}O$ has been observed as an excellent photocatalyst, and shown promising results for the degradation of Cr(VI).

Keywords: Metal oxides, Semiconductors, Zinc Oxide, Magnesium oxide, Crystallite size, Band gap, Photo-catalysis, Hexavalent and trivalent Chromium, Photo catalyst.

INTRODUCTION

In recent years, the world, mostly the advanced nations, facing tremendous issues like energy shortage and environmental problems related to the remediation of hazardous waste and polluted air and water contaminants. One of the promising solutions for the above-mentioned problems is "Semiconductor photo-catalysis". Since it is a "green technology" for the splitting of H_2O, inactivating/eliminating all kinds of organic and inorganic contaminants in the presence of sunlight under ambient conditions[1,2]. Photo-catalysis is the process of employing a catalyst that is used for enhancing chemical reactions in the presence of light. A photocatalyst is a material that absorbs light and produces electron-hole pairs that facilitate chemical changes of the participants and reproduces its chemical composition after each interval of interactions with light[3–8]. The photocatalysts based on semiconductor metal oxides are usually used as activators that catalyze the radical chain reaction in photocatalytic oxidation. Also these materials can be used in the photo catalytic treatment of dyes in waste-water, due to low cost and other tunable properties,

without any significant loss in their photo catalytic activity[9].Nanoparticles of metal oxide semiconductors have achieved various functionalities that are not experimentally found in bulk materials and have been studied extensively due to their unique structural, optical, electronic, magnetic, photo catalytic, antitumor, antimicrobial, wound healing and anti-inflammatory properties[10-21]. Over the last 10 years, there is an exponential growth in the scientific and engineering interest on semiconductor photo-catalysis[21]. Out of this practical interest, there is a comprehensive research effort in developing novel photocatalytic materials for better efficiency under solar illumination. Low-cost metal oxide semiconductor photocatalysts with higher photocatalytic efficiency offer enormous potential applications for the purification of four elements in "five great elements" such as earth, water, air and space along with the conversion of photon energy into chemical energy. As a wide band gap (E_g=3.37 eV at 300 K) semiconductor with large exciton binding energy (60 MeV)[23], Zinc oxide (ZnO) is a promising and versatile material, that has been intensively studied in the field of blue-violet light emitting diodes (LEDs), ultraviolet detectors, solar cells, field-effect transistors (FETs), sensors, and photo-catalysis[23]. Band-gap engineering is important in tuning the optical, magnetic and electrical properties and to develop new structural designs[23,24]. In this context, Magnesium oxide (MgO) is one of the promising candidates for altering (increasing) the E_g of ZnO due to small lattice mismatch of MgO with ZnO. Being non-toxic and multi-functional, ZnO is an effective material in green technology[19,22]. Accordingly, from the viewpoint of semiconductor photochemistry, the role of photocatalyst is to accelerate specific redox reaction in the presence of irradiated semiconductors In general, the photochemical activities are based on the direct excitation of the target molecules by visible light or UV. Absorbing materials are used in photo catalytic reactions, which are energized by light and are able to transfer electrons from their excited states to the molecules to be converted. Electrons which is in the conduction band may photo catalytically reduce the organic pollutant[25,26]. A considerable amount of chromium (Cr) is widely used in several industries such as stainless steel, plating, leather tanning, mining, paint making and others[21,26]. Chromium metal is an essential trace element for human health. However, the raw industrial wastes contain the hexavalent chromium, Cr(VI), which is highly toxic, carcinogenic, may cause pulmonary congestions, and liver damage[21,26]. Since it is highly toxic in nature, Cr(VI) has been considered as one of the most noxious wastes that are to be removed especially from drinking water. According to the World Health Organization (WHO), the limit of Cr(VI) in drinking water is 0.05ppm[21]. On the other hand, trivalent chromium, Cr(III), is eco-friendly. It is an important trace element for regulating the insulin function in the human body. Consequently, the reduction of Cr(VI) to Cr (III) is crucial in environmental issues[21].

There are different chemical methods for reducing Cr(VI). The photocatalytic reduction with semiconducting metal oxides is regarded as a smart green technology not only because of its low cost, high effectiveness and non-usage of any harmful reducing agents but also the reduction proceeds without the production of any secondary pollutants. A variety of semiconducting catalysts such as TiO_2, ZnO, ZnS, $ZnIn_2S_4$, and$La_2Ti_2O_7$ have been used for the photoreduction of Cr (VI)[21,27,28]. Upon irradiation with light/UV, in these II-VI metal oxide semiconducting materials, electrons move from valence band (VB) to conduction band (CB) leaving holes in VB[21]. Electrons in the conduction band photocatalytically reduce the organic/inorganic pollutant. In the industrial sector, the installation cost of such photocatalytic reactors is very high and the main problem associated with this reactor configuration is the issue of scale-up for commercial use purposes[29]. With a clear objective in achieving a cost-effective and easily assembled unit, a new photoreactor (built in-house) is developed with UV LED strip as the light source. Simultaneous monitoring of multiple analyses can be easily done with this system. In this present work, we synthesized $Mg_xZn_{(1-X)}O$. The structural and optical properties of the obtained materials were characterized. Also, we are contented to report for the first time that we have developed a new low-cost photocatalytic reactor (built in-house) with UV LED light strip as a light source.

EXPERIMENTAL

Materials
Analytical grade chemicals were used in this experiment without any further purification. Zinc sulphate($ZnSO_4.7H_2O$),sodium hydroxide (NaOH), magnesium sulphate($MgSO_4.7H_2O$), cetyl

trimethylammonium bromide (CTAB), deionized water, nitric acid (HNO_3),ethanol (C_2H_5OH, >99%), isopropyl alcohol (C_3H_8O)and Whatman No. 40 filter paper were used in this experiment. All the chemicals are of purity ≥ 98% and were obtained from Sigma-Aldrich.

Synthesis of $Mg_xZn_{(1-x)}O$(x=0, 1, 5 and 10%) Nanoparticles
The scheme that was followed for the synthesis of our compounds is mechanic assisted chemical co-precipitation technique[30] in which a surfactant was also used.

General Procedure
For the synthesis of zinc oxide, the required aqueous solution of zinc sulphate was prepared. To this, a solution contains both NaOH and CTAB was added dropwise with constant stirring. After the addition, stirring was continued for 2 hours in order to ensure the completeness of the reaction. The turbid solution obtained was kept undisturbed for the settlement of the precipitate and the supernatant was discarded. The precipitate, zinc hydroxide ($Zn(OH)_2$),obtained was thoroughly cleaned washing with deionized water, ethanol and acetone to remove unwanted salt and impurities. The prepared $Zn(OH)_2$ was heated at 150ºC for two hours in order to convert it into ZnO. It was then allowed to cool and ground in order to assist for size reduction[30]. The chemical equations representing the preparation as follows:

$$ZnSO_4.7H_2O + 2NaOH \rightarrow Zn(OH)_2 + Na_2SO_4 + 7H_2O$$
$$Zn(OH)_2 \rightarrow ZnO + H_2O$$
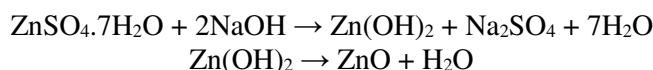
To prepare the doped samples, i.e.$Mg_xZn_{(1-x)}O$, different molar concentrations of $MgSO_4.7H_2O$were added to the solution of $ZnSO_4.7H_2O$ followed by a solution contains both NaOH and CTAB. The flow chart of the chemical reaction isgivenintheFig.-1.
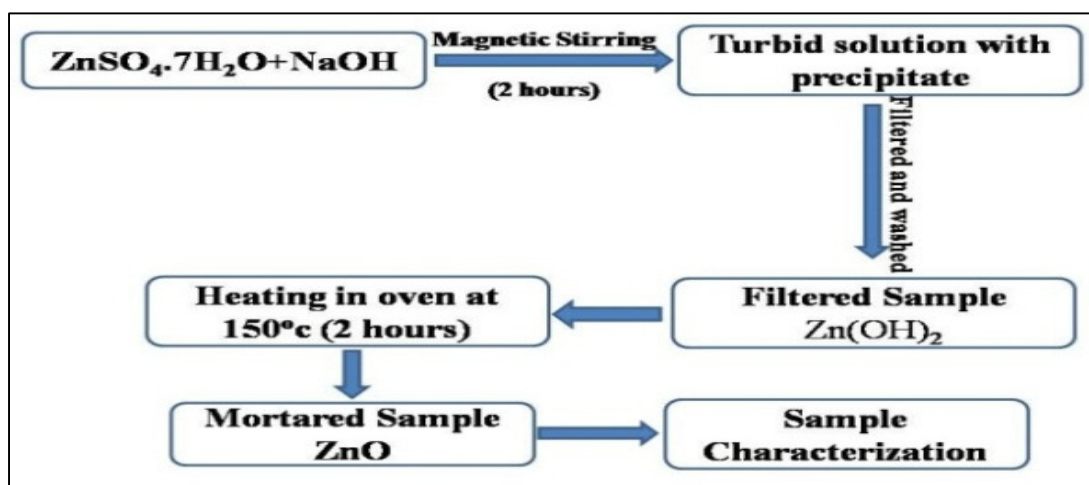

Fig.-1: The Flow Chart of the Chemical Reaction

Detection Method
In order to investigate various properties of the prepared samples, they have to be characterized using various techniques which can give information on their structural and optical properties. In the present work, the structural analysis of the prepared samples was carried out by X-ray diffraction (XRD with Cu Kα, λ = 1.5405 Å) and optical characterization was done through UV/Vis spectroscopy. In our studies, we made use of Philip PW1700 XRD and JASCO UV-Vis NIR spectrometer (V-670).

Instrumentation–Photocatalytic Reactor
A line diagram of the photoreactor assembly is shown in Fig.-2. The photoreactor was built in-house, with a clear objective in achieving a cost-effective and easily assembled unit, for simultaneous monitoring of multiple analyses. The housing of the unit was made of the galvanized sheet which was hammered down to a neat cabin of 2×1×2 feet dimension. The cabin was fit with a door of the same material to enable easy

handling of the sample. The inside of the cabin, including the door, was decorated with 2'' thermal insulation with proper rubber beadings to win a compact setting and minimize any heat loss that may occur during operation. The inner side of the cabin was cemented with a UV LED strip (150V-265V AC input, power 0.2 W) in series of three tiers of equal dimensions. No strip was affixed on the roof of the cabin in order to avoid any discomfort. A magnetic stirrer was placed inside the cabin to agitate the contents of the 100 mL borosil® beaker, which was used as the reactor. The open beaker attracted maximum radiation and the thin walls facilitated in this action. The whole of the cabin was maintained at a static temperature of 296 K with the help of an insulated-ducted air-heat exchanger of 300 kcal/h capacity. This profusely helped to sufficiently cool the reactor and maintain uniform temperature distribution without any gradient formation.
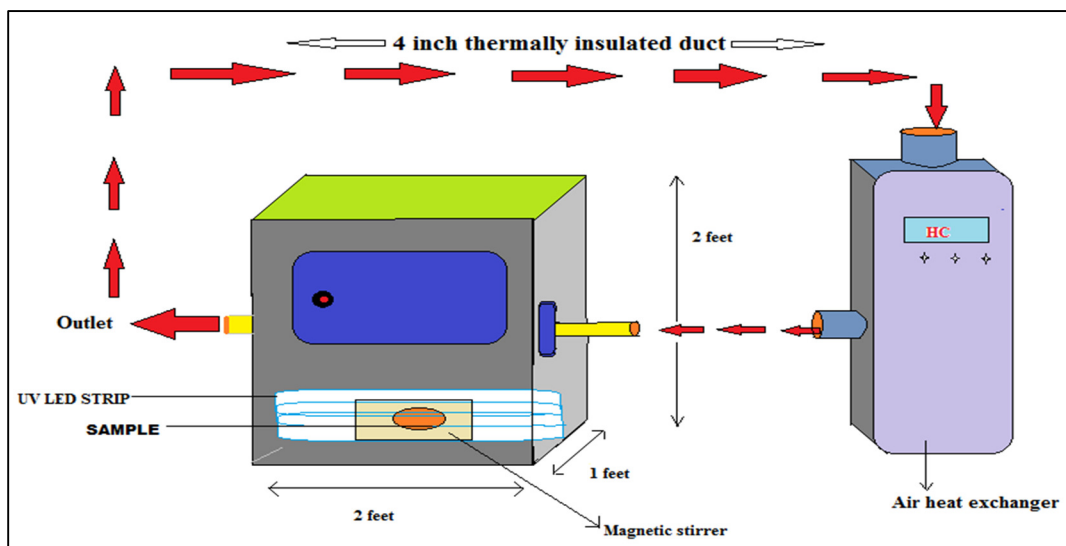

Fig.-2: Line-Diagram of the Photo-Reactor Assembly

Analytical Discussion
The photocatalytic experiments were studied under UV light using RGB 300 UV LED strip (150V-265V AC input).For every experiment, 100 mL of 50 ppm Cr(VI) solution containing 10mL of oxalic acid as hole scavenger was taken in a 500 mL beaker. The photocatalyst, 20 mg, was added to the solution and was shaken in an orbital shaker at 200 rpm. Initially, the solution was shaken in dark for 15 min to reach an adsorption-desorption equilibrium of Cr(VI) over the catalyst. This was followed by irradiation of UV light under aerobic condition. The aliquots were collected in a regular interval during photoreduction. Diphenylcarbazide (DPC) was used as the indicator to follow the photocatalytic reaction. The residual Cr(VI) concentration was determined using UV-Vis spectrophotometer at 540 nm after complexation with DPC. This is repeated for Mg-doped samples.

RESULTS AND DISCUSSION

The structure of the samples was characterized by XRD. The XRD patterns of $Mg_xZn_{(1-x)}O$ samples are shown in the Fig.-3. The peaks at 31.5º, 34.28º, 36.16º, 47.45º, 56.45º, 62.8º and 67.8º indicate that the samples are highly crystalline. Comparing with JCPDS data 36-1451, lattice planes are identified as (100), (002), (101), (102), (110), (103) and (112), respectively, indicating hexagonal wurtzite structure of ZnO. The broadening of the peaks gives an idea about the small particle size of the synthesized ZnO.
From the XRD data, it is clear that there is a shift of diffraction peaks towards higher angles with the increase in dopant concentration. This indicates that Zn^{2+} is substituted by Mg^{2+} in the host lattice. The 'a' and 'c'-axis lattice constants for (100) and (002) peaks were calculated[31] using the relations, $a = \frac{\lambda}{\sqrt{3}\sin\theta}$ and $c = \frac{\lambda}{\sin\theta}$.The calculated lattice parameters are given in the Table-1. The lattice constants 'a' and 'c' of $Mg_xZn_{(1-x)}O$ are similar to pure ZnO at room temperature [JCPDS card no. 36–1451]. The lattice

constant 'a' and 'c' are reduced monotonically, i.e., 'a' is reduced from 3.2729 to 3.2445 Å and 'c' is reduced from 5.3446 to 5.1977 Å. It is owing to the fact that the Mg^{2+} replaced $Zn^{2+}$from ZnO and lodged itself in the interstitial position. Also, the decrease of lattice parameters is ascribed to comparatively lower ionic radii of Mg^{2+} compared to Zn^{2+} ions [32].
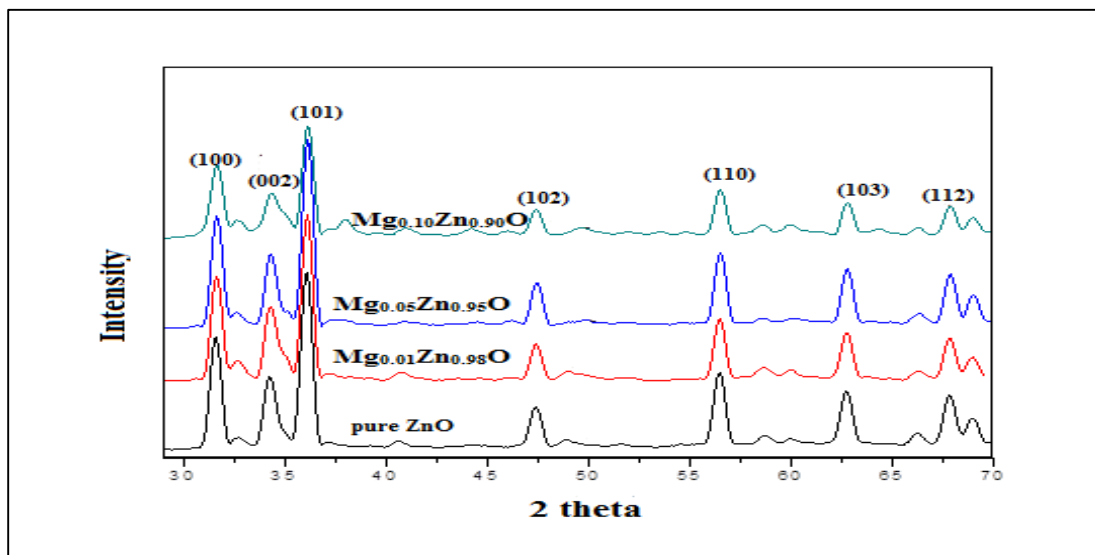

Fig.-3: XRD Pattern of $Mg_xZn_{(1-x)}O$ Nanoparticles for Different Doping Concentrations

Table-1:The Calculated Lattice Parameters for $Mg_xZn_{(1-x)}O$

Sample	Lattice parameter (a)Å	Lattice parameter (c)Å	Volume(Å^3)
ZnO	3.2729	5.3446	49.5788
$Mg_{0.01}Zn_{0.99}O$	3.2718	5.3412	49.5145
$Mg_{0.05}Zn_{0.95}O$	3.2684	5.3373	49.3746
$Mg_{0.10}Zn_{0.90}O$	3.2445	5.1977	47.3840

The average crystallite size (D) was calculated using the Scherer's formula[24] given as $D = \frac{0.89\lambda}{\beta\cos\theta}$, where λ=1.514×10^{-10}m and β is full width at half maximum (FWHM).The calculated crystallite sizes of the samples are tabulated in Table-2.

Table-2: Calculated Crystalline Size for the Prepared Samples

Sample	Peak(deg)	FWHM(β)	Crystalline Size(D) nm	Plane
ZnO	36.0334	0.5457	13.8465	101
$Mg_{0.01}Zn_{0.99}O$	36.0323	0.4518	16.7243	101
$Mg_{0.05}Zn_{0.95}O$	36.5740	0.5160	14.4968	101
$Mg_{0.10}Zn_{0.90}O$	36.6398	0.5100	14.9221	101

As Mg is doped, it is seen immediately that the size of the particles increases. The crystallite size as a function of dopant concentration is shown in the Fig.-4.It can also be seen that the crystallite size decreases up to 5% Mg-doped ZnO and then remains almost constant with the increase in Mg concentration. The gradual increase of Mg doping progressively reduces the concentration of zinc in the system. The reason for the decrease in size can be explained in two ways. Firstly, the decrease in crystal size can be attributed to the formation of Mg-substituted ZnO (Mg-O-Zn) solid solution which inhibits the growth of crystal grains[33]. Secondly, the decrease in crystallite size as a function of Mg content can be explained by the Zener pinning effect[34]. There are a variety of inherent defects present in ZnO with different ionization energies such as oxygen vacancy (V_O), zinc vacancy (V_{Zn}), oxygen interstitials (O_i) and zinc interstitials (Zn_i)[23]. Due to these crystal defects and imperfections, the expansion of grain boundaries gets restricted in a crystal which is called Zener pinning effect[34]. In the present study, after

1495

doping, the number of V_O present in the ZnO lattice may be increased. These oxygen vacancies may restrict the growth of the crystallites owing to the Zener pinning effect.
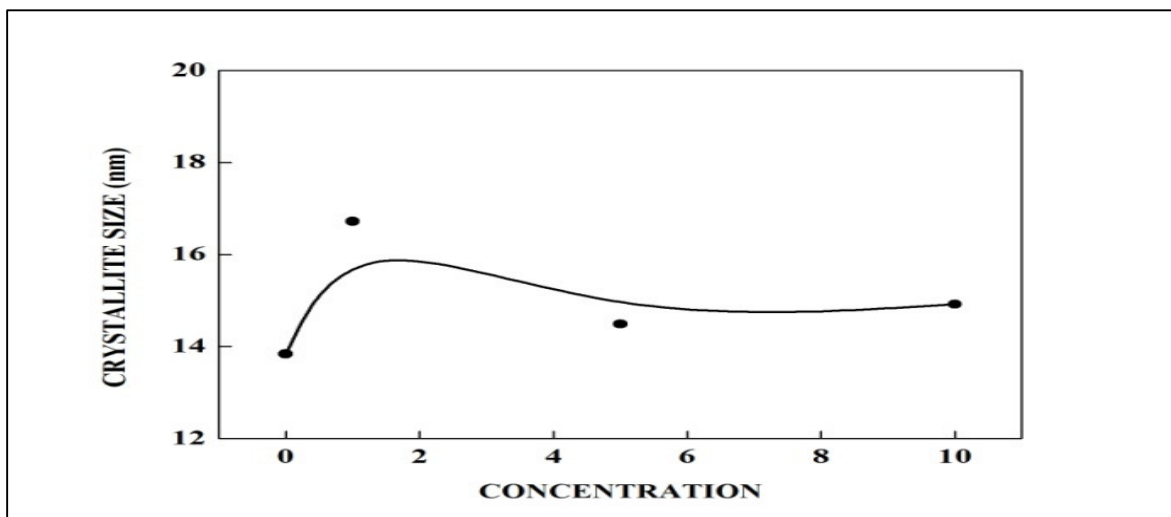

Fig.-4:Comparison of the Variation of Crystallite Size with Concentration of Mg

UV-Vis Characterization

The room temperature optical measurements were performed using a UV-visible-near infrared spectrophotometer. The absorbance spectra of $Mg_xZn_{(1-x)}O$ nanoparticles are shown in the Fig.-5 and is observed that the absorbance wavelength decreases(blue shift) with an increase in doping concentration. This indicates the widening of E_g, which agrees with the reported experimental results[32,33,35]. The room temperature E_g for ZnO can be tuned to fit the desired applications by doping with suitable divalent elements without affecting the charge carrier concentrations in ZnO. In particular, Mg doping increases the E_g further into the UV range and it results in a blue shift in the absorption spectra.
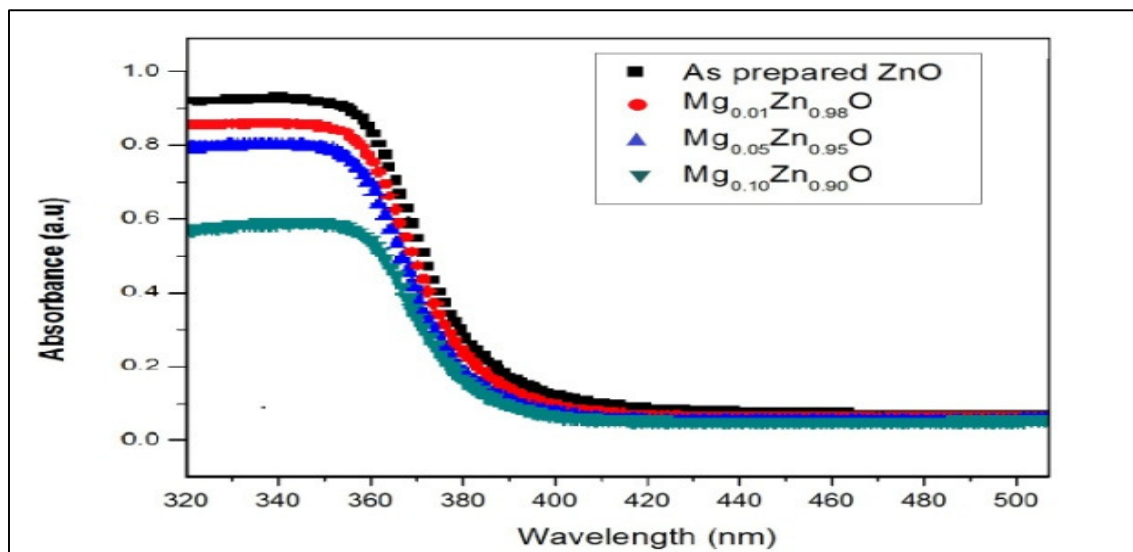

Fig.-5: The Absorbance Spectra of ZnO and Mg doped ZnO Samples

The Tauc plot for $Mg_xZn_{(1-X)}O$ samples in comparison with ZnO is given in the Fig.-6. The E_g obtained from the plot is tabulated in the Table-3.

The shifting of absorbance spectra to the shorter wavelength depends upon a number of reasons. Blue shift commonly occurs when the particle size is decreased. When the Bohr's radius is higher than the particle size, this shift can be described by the effect of quantum confinement[33]. However, the crystallite

1496

size of all $Mg_xZn_{(1-x)}O$ nanoparticles prepared in this studies is further than the Bohr's radius, thus the change in E_g values might be influenced by other parameters. Here, the increase in a blue shift or the band gap can be explained on the basis of Burstein-Moss effect[32]. ZnO is an n-type semiconductor and the Fermi level lies inside the conduction band (CB). Doping of Mg donates a large number of electrons due to the lesser electron affinity of MgO in contrast to ZnO. Consequently, the Fermi level for $Mg_xZn_{(1-X)}O$ samples is located at a higher position. Hence, the blue shift or increase in E_g is due to the radiative recombination of these electrons.
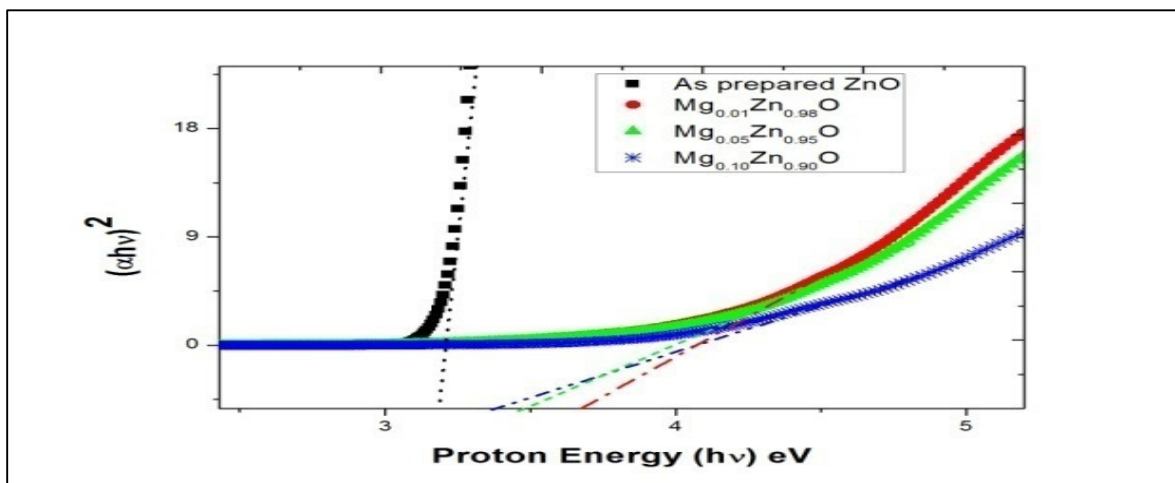

Fig.-6: Optical Absorption Spectra (Tauc plot) of ZnO and Mg-doped ZnO samples

Photocatalytic Study

Upon irradiation, the electrons jump from VB to CB, leaving holes in VB. The reduction potential for Cr(VI)/Cr(III) with respect to a normal hydrogen electrode (NHE) is 1.33 V. If the chosen catalytic material's CB edge is above 1.33 V, the electron, which is in the CB may photocatalytically reduce Cr(VI) to Cr(III)[21]. Photocatalytic degradation of Cr was chosen as a reference and the characteristic absorption of the Cr seen at the UV-Visible range was selected for monitoring the photocatalytic reduction process of ZnO nanoparticles. Fig.-7 and 8 represent the typical curves for the normalized concentrations of the Cr solution as a function of UV irradiation time over the as-prepared ZnO and $Mg_{0.01}Zn_{0.99}O$ nanoparticles. In comparison with slow degradation process of the Cr under the UV irradiation with undoped ZnO nanoparticles, adding of Mg-doped ZnO nanoparticles markedly accelerated the reduction of Cr with increasing Mg concentration.
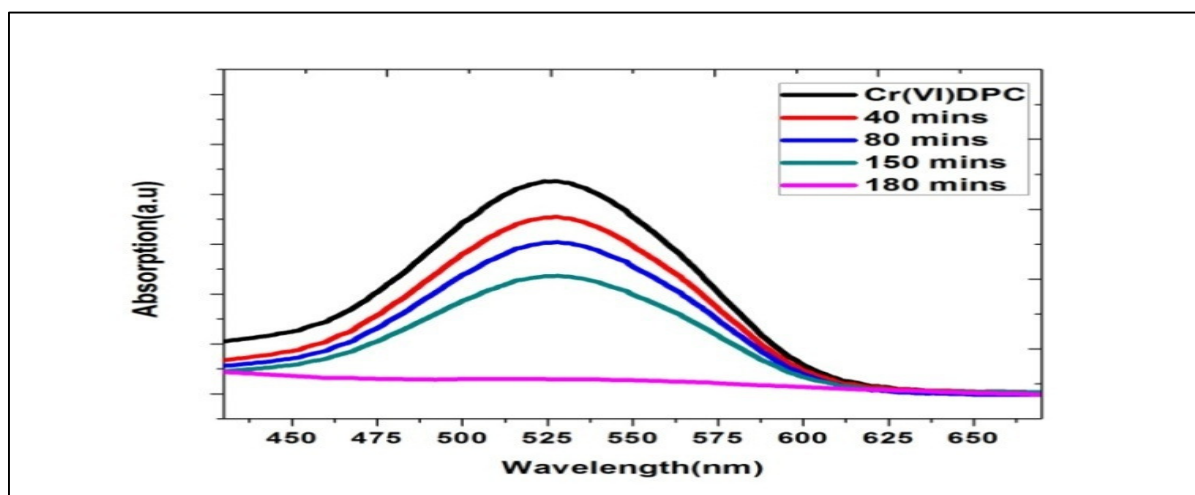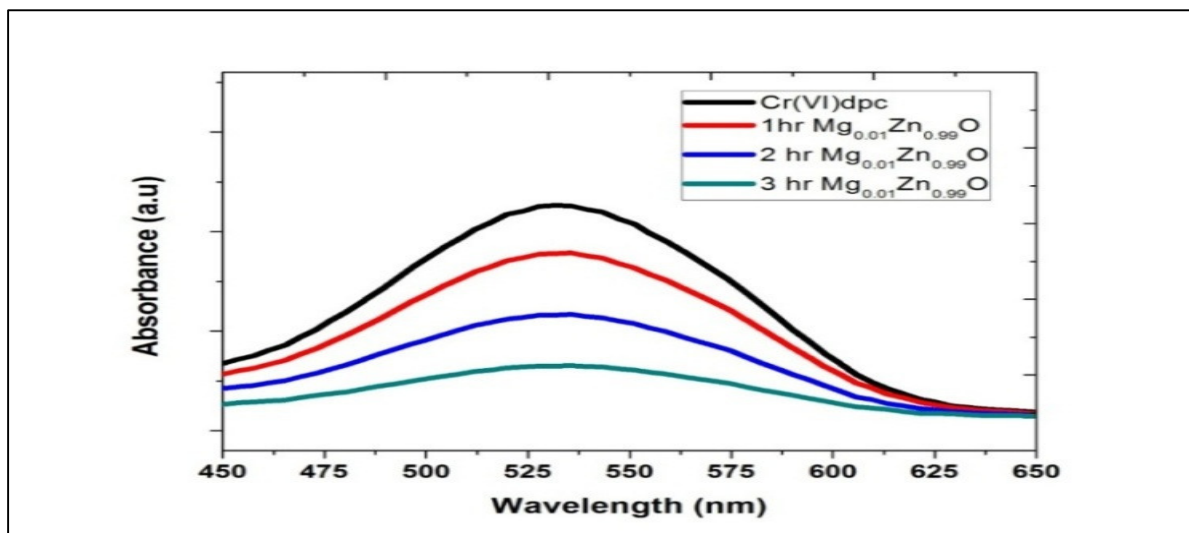

Fig.-7: Optical Absorbance Spectra of Photocatalytic Degradation of Cr(VI) Solution as a Function of UV irradiation on ZnO

1497

Table-3: The E_g determined from the Tauc Plot

Sample	Energy Gap(eV)
ZnO	3.28
$Mg_{0.01}Zn_{0.99}O$	3.38
$Mg_{0.05}Zn_{0.95}O$	3.44
$Mg_{0.10}Zn_{0.90}O$	3.69

Fig.8-: Optical absorbance spectra of photocatalytic degradation of Cr(VI) solution as a function of UV irradiation on $Mg_{0.01}Zn_{0.99}O$

Effect of Doping on Photo-Catalysis

From Fig.-9 showing the photocatalytic degradation of Cr(VI) solution as a function of UV irradiation for a constant time (120 min) on $Mg_xZn_{(1-x)}O$ nanoparticles, it is observed that the photocatalytic activity is increasing as the doping concentration increases.
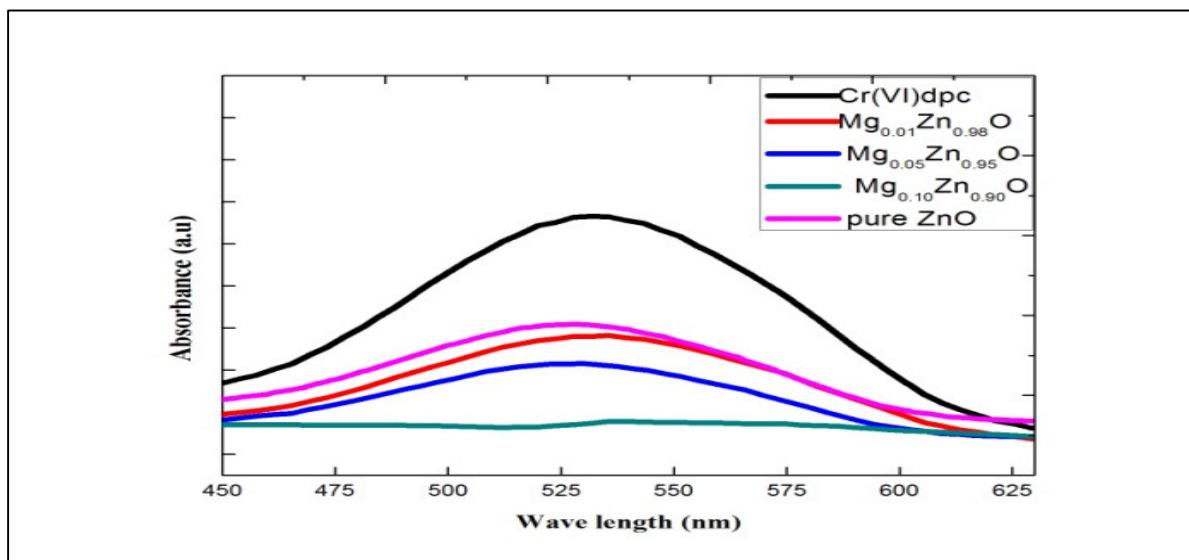
Fig.-9:Room temperature optical absorbance spectra of photocatalytic degradation ofCr(VI) solution as a function of UV irradiation for a constant time (120 min) on $Mg_xZn_{(1-x)}O$ nanoparticles

This acceleration in photocatalytic activity (as doping concentration increases) could be due to the presence of vacancies and trace metal ions doped in the ZnO matrix which can effectively trap the photo-generated hole-electron pairs with the help of hole scavengers like oxalic acid[21].The superficial potential

1498

trap of photo-generated electron-hole pairs lengthen the lifetime of electrons and holes and increases photocatalytic activity[21,27,28]. Therefore, ZnO and $Mg_xZn_{(1-x)}O$ have been observed as excellent photocatalysts. The development of such photocatalysts is considered as a promising material in the large-scale utilization of heterogeneous photo-catalysis via visible or UV to deal with contaminated water and other environmental pollutions.

CONCLUSION

In this present work, we synthesized undoped and Mg-doped ZnO nanoparticles by the co-precipitation method. From XRD analysis, it is seen that Mg^{2+} ions exactly replaced the Zn^{2+} ions without affecting the crystal structure. We noticed that E_g of the ZnO nanoparticle varies with Mg doping. These synthesized $Mg_xZn_{(1-x)}O$ samples have been observed as excellent photocatalysts. The $Mg_xZn_{(1-x)}O$ photocatalyst showed promising results for the degradation of Cr(VI) for detoxification and environmental remediation.

ACKNOWLEDGMENT

REFERENCES

1. Andrew Mills and Stephen Le Hunte, *Journal of Photochemistry and Photobiology A: Chemistry*, **108**, 1(1997), **DOI:**10.1016/S1010-6030(97)00118-4.
2. Monu Bhardwaj and Neelam, *Journal of Basic and Applied Engineering Research*, **2(22)**,1957(2015)
3. T. A. Arun, Chacko, D. K., Madhavan, A. A., Deepak, T. G., Anjusree, G. S., Sara, T., Ramakrishna, S., Nair, S. V. and A. Nair, S., *RSC Advances*, **4**, 1421(2014), **DOI:**10.1039/C3RA45021J .
4. P. Amornpitoksuk, S. Suwanboon, S. Sangkanu, A. Sukhoom, N. Muensitand J. Baltrusaitis, Powder Technol.,**219**, 158(2012), **DOI:** 10.1016/j.powtec.2011.12.032.
5. Sumetha Suwanboon, Pongsaton Amornpitoksuk, Apinya Sukolrat and Nantakan Muensit, *Ceramics International*, **39**, 2811(2013), **DOI:** 10.1016/j.ceramint.2012.09.050.
6. K. Ravichandran, P. Sathish, S. Snega, K. Karthika, P. V. Rajkumar, K. Subha and B. Sakthivel, *Powder Technology,* **27**4, 250(2015), **DOI:** 10.1016/j.powtec.2014.12.053.
7. K. Ravichandran, S. Snega, N. Jabena Begum, L. Rene Christena, S. Dheivamalar and K. Swaminathan, *Philosophical Magazine*, **94**, 22, 2541(2014), **DOI:** 10.1080/14786435.2014.921349.
8. Adil and Al-Mayouf, *Journal of Saudi Chemical Society*, (2015), **DOI:** 10.1016/j.jscs.2015.04.003.
9. Zhibin Wu, Xingzhong Yuan, Jin Zhang, Hou Wang andLongbo Jiang, Guangming Zeng, *Chem. Cat. Chem.*, **9**, 1(2016), **DOI:** 10.1002/cctc.201600808.
10. Sreekanth K. Mahadeva, Quan, Z. Y., Fan, J. C., Albargi, H. B., Gehring, G. A., Riazanova, A., Belova, L., and Rao, K. V., In Symposium F-Oxide Semiconductors and Thin Films, **1494**, 115(2013), **DOI:** 10.1557/opl.2013.260.
11. Uma Maheswari, A., Saravana Kumar, S. and Sivakumar, M., J. Nanosci. Nanotechnol., **13(6)**, 4409 (2013), **DOI:**10.1166/jnn.2013.7150.
12. Sreekanth K. Mahadeva, Fan, J., Biswas, A., Rao, G. M., Sreelatha, K. S., Belova, L., and K Rao, V., Materials Express, **3**, 328(2013), **DOI:** 10.1166/mex.2013.1131.
13. Uma Maheswari A., Mohan S. R., Saravana Kumar S. and Sivakumar M., *Ceram. Int.*, **40**, 5 6561(2014), **DOI:** 10.1016/j.ceramint.2013.11.109.
14. Sreekanth K. Mahadeva, Fan, J., Biswas, A., Sreelatha, K. S., Belova, L., and Rao, K. V., *Nanomaterials,* **3**, 486(2013), **DOI:** 10.3390/nano3030486.
15. P. T. Sudheesh Kumar, Lakshmanan, V. K., Anilkumar, T. V., Ramya, C, Reshmi, P., Unnikrishnan, A. G, Nair, S. V, and Jayakumar, R., *ACS Applied Materials and Interfaces*, **4**, 2618(2012), **DOI:** 10.1021/am300292v.
16. B. H. N. Reddy, T. M. Mohan Kumar, and Lakshmi, V. V., *Journal of Bionanoscience*, **11**, 59(2017), **DOI:** 10.1166/jbns.2017.1412.
17. Rex Jeya Rajkumar S, MSA Muthukumar Nadar and Paulraj Mosae Selvakumar, *Glob. J. Nanomed.*, **3**, 1(2017), **DOI:**10.19080/GJN.2017.03.555605.

18. D. Saratchand A., Sreekanth K. M., Krishnan N. Cherupally, and Rao, K. V., *Journal of Cancer Therapy*, **2**, 666(2011), **DOI:** 10.4236/jct.2011.25089.
19. B. Das, M. I. Khan, R. Jayabalan, S. K. Behera , S.I.Yun , S.K.Tripathy , A.Mishra, *Sci. Rep*., **6,** 36403(2016), **DOI:** 10.1038/srep36403.
20. Sangeetha Gunalana , Rajeshwari Sivaraja, and Venckatesh Rajendran*, Progress in Natural Science: Materials International*,**22(6)**, 693(2012), **DOI:** 10.1016/j.pnsc.2012.11.015.
21. Ravikiran Nagarjuna, Swapna Challagulla, Ramakrishnan Ganesan and Sounak Roy, *Chemical Engineering Journal*, **308,** 59(2017), **DOI:** 10.1016/j.cej.2016.09.044.
22. K. T. Shalumon, Anulekha, K. H., Nair, S. V., Chennazhi, K. P., and Jayakumar Rangasamy, *International Journal of Biological Macromolecules*, **49**, 247(2011), **DOI:** 10.1016/j.ijbiomac.2011.04.005.
23. J.C. Fan, K.M. Sreekanth, Z. Xie, S.L. Chang, and K.V. Rao, *Progress in Materials Science*, **58(6)**, 874(2013), **DOI:** 10.1016/j.pmatsci.2013.03.002.
24. Sreekanth K. Mahadeva, Ph. D. Thesis, Department of Material Science and Engineering, KTH-The Royal Institute of Technology, Stockhom, Sweden,(2013)
25. S. S. Shinde , C. H. Bhosaleand K. Y. Rajpure, *Catalysis Reviews: Science and Engineering*, **55(1)**, 79(2013), **DOI:** 10.1080/01614940.2012.734202.
26. Francesco Parrino and Leonardo Palmisano, *Mini-Reviews in Organic Chemistry*, **15**, 157(2018), **DOI:** 10.2174/1570193X14666171117151718.
27. G. Cappelletti, C.L. Bianchi, and S. Ardizzone, *Appl. Catal. B: Environ.,* **78**, 193(2008), **DOI:** 10.1016/j.apcatb.2007.09.022.
28. Y. Ku, and I.L. Jung, Water Res.,**35,** 135(2001), **DOI:** 10.1016/S0043-1354(00)00098-1.
29. Mukherjee, P.S. and A.K. Ray, *Chemical Engineering and Technology*, **22(3)**, 253(1999), **DOI:** 10.1002/(SICI)1521-4125.
30. S. Das and V. C. Srivasatava, *Smart Science*, **4(4)**, 190(2016), **DOI:** 10/1080 /23080477.2016.1260425.
31. F. K. Shan, B. I. Kim, G. X. Liu, Z. F. Liu, J. Y. Sohn, J. Lee, B. C. Shin, and Y. S. Yu, *J. Appl. Phys.,* **95**, 4772 (2004), **DOI:**10.1063/1.1690091.
32. Parmod Kumar, Hitendra K. Malik, Anima Ghosh, R. Thangavel, and K. Asokan, *Appl. Phys. Lett.,* **102**, 221903 (2013), **DOI:** 10.1063/1.4809575.
33. S. Suwanboon, P. Amornpitoksuk, A. Haidoux, J.C. Tedenac, *Journal of Alloys and Compounds*, **462,** 335(2008), **DOI:**10.1016/j.jallcom.2007.08.048.
34. R.W. Kelsall, I.W. Hamley, and M. Geoghegan, Nanoscale Science and Technology, John Wiley and Sons, West Sussex, (2005)
35. Samson B. Woodley, Alexey A. Sokol, Richard A. Catlow, Abdullah A. Al-Sunaidi, and Scott M. Woodley, *J. Phys. Chem. C*,**117**, 27127(2013), **DOI:** 10.1021/jp4084635.

[RJC-4000/2018]